

Supplementary information

Microwave-assisted synthesis of nanocrystalline Cd_{0.6}Zn_{0.4}S photocatalyst with twin structure: effect of SDBS and enhanced performance for H₂ evolution

Yao-Guang Yu,^a Gang Chen,*^a Yan-Song Zhou,^a Yu Wang^a and Chong Wang^b

^a Department of Chemistry, Harbin Institute of Technology, Harbin 150001, P. R. China, E-mail: gchen@hit.edu.cn; ygyu@hit.edu.cn, Tel: +86-451-86403117

^b School of Chemical Engineering and Technology, Harbin Institute of Technology, Harbin 150001, P. R. China

Table of contents

Characterization of photocatalysts	2
Details of molecular dynamics simulation.....	2
Photocatalytic reactions	3
Table S1	4
Reference	5
Figure S1–S12.....	6

Characterization of photocatalysts

Crystal structures of as-prepared products were investigated by a Rigaku D/max-2000 diffractometer with CuK α radiation ($\lambda = 0.15406$ nm). The microstructure and composition analysis were conducted on a field emission scanning electron microscope (FESEM, FEI QUANTA 200F) working at 30 kV and a transmission electron microscope (TEM, FEI Tecnai G²) equipped with an energy-dispersive X-ray spectrometer (EDS) working at 300 kV. High angle annular dark field (HAADF) imaging was obtained in scanning TEM (STEM) mode. BET specific surface areas and pore volumes were calculated from nitrogen adsorption/desorption isotherms determined at 77 K using an AUTOSORB-1-MP surface analyzer (the sample was outgassed under vacuum at 150 °C). UV-vis diffuse reflectance spectra were acquired by a spectrophotometer (TU-1900) and were converted from reflection to absorbance by the standard Kubelka-Munk method. BaSO₄ was used as the reflectance standard. Infrared analysis was identified by a FTIR spectrometer (Shi-madzu) in the range of 400–4000 cm⁻¹ with the samples mulled in KBr wafers.

Details of molecular dynamics simulation

MD simulations of the interaction between SDBS and the (111) surface of Cd_{0.5}Zn_{0.5}S solid solution were carried out in a simulation box (1.58 nm × 3.15 nm × 7.85 nm) with periodic boundary conditions using Materials Studio 5.0 version (from Accelrys Inc). Due to the asymmetric structure between the top and the bottom of the supercell, a dipole correction was introduced to avoid any arbitrary boundary effect.¹ The box consisted of a (111) surface of cubic Cd_{0.5}Zn_{0.5}S solid solution, two liquid phases and a vacuum layer of 10 nm height. One liquid phase was near the (111) surface of Cd_{0.5}Zn_{0.5}S solid solution containing a SDBS molecule and 200 methanol molecules with density of 0.9 g·cm⁻³, while another one was fixed below the vacuum layer containing 50 methanol molecules with density of 0.8 g·cm⁻³ in order to prevent the dipole field effect. The MD simulation was performed at 339 K, NVT ensemble and COMPASS force field, with the time step of 1 fs and simulation time of 0.5 ns.

The interaction energy $E_{(111)\text{-SDBS}}$ was calculated as:

$$E_{(111)\text{-SDBS}} = E_{\text{total}} - E_{(111)} - E_{\text{SDBS}}$$

Here, E_{total} is the total energy of (111) surface of $\text{Cd}_{0.5}\text{Zn}_{0.5}\text{S}$ solid solution together with the adsorbed SBDS molecule; $E_{(111)}$ and E_{SDBS} are the total energy of the $\text{Cd}_{0.5}\text{Zn}_{0.5}\text{S}$ crystal and free SBDS molecule, respectively.

Photocatalytic reactions

The photocatalytic reaction was performed in a closed gas-circulation system with a side window. The photocatalyst powders (0.015 g) were dispersed by ultrasonication for 30 min in an aqueous solution (400 mL) containing Na_2SO_3 ($0.6 \text{ mol}\cdot\text{L}^{-1}$) and Na_2S ($0.4 \text{ mol}\cdot\text{L}^{-1}$) as electron donors. Nitrogen was purged through the system for 30 min to remove oxygen before reaction. The reaction was carried out by irradiating the suspension with light from a 300 W Xe lamp which was equipped with an optical filter ($\lambda \geq 400 \text{ nm}$) to cut off the light in the ultraviolet region. The amount of produced H_2 was measured by gas chromatography (Agilent 6820) with a thermal conductivity detector (TCD) and Ar was used as the carrier gas.

Table S1 $\text{Cd}_x\text{Zn}_{1-x}\text{S}$ photocatalysts synthesized through various synthetic methods for photocatalytic H_2 production

photocatalyst	synthetic method	mass (mg)	light source	incident light	activity ($\mu\text{mol}\cdot\text{h}^{-1}\cdot\text{g}^{-1}$)	aqueous solution	ref
$\text{Cd}_{0.5}\text{Zn}_{0.5}\text{S}$ (with twins)	Precipitation -hydrothermal	100	300W Xe lamp	$\lambda \geq 430$ nm	17900	0.35 M Na_2S and 0.25 M Na_2SO_3	2
$\text{Cd}_{0.6}\text{Zn}_{0.4}\text{S}:$ 2%La	Solvothermal	15	300W Xe lamp	AM1.5 and $\lambda \geq 400$ nm	92700	0.6 M Na_2S and 0.8 M Na_2SO_3	3
$\text{Cd}_{0.7}\text{Zn}_{0.3}\text{S}$	Coprecipitation	100	300W Xe lamp	visible light	<i>ca.</i> 350	0.05 M Na_2S and 0.02 M Na_2SO_3	4
$\text{Cd}_{0.8}\text{Zn}_{0.2}\text{S}$	Cation exchange	50	350W Xe lamp	$\lambda \geq 400$ nm	2128	0.1 M Na_2S and 0.04 M Na_2SO_3	5
$\text{Cd}_{0.5}\text{Zn}_{0.5}\text{S}$	Thermolysis	50	350W Xe lamp	$\lambda \geq 400$ nm	7420	0.44 M Na_2S and 0.31 M Na_2SO_3	6
$\text{Cd}_{0.6}\text{Zn}_{0.4}\text{S}-0.6$	Microwave-assisted synthesis	15	300W Xe lamp	$\lambda \geq 400$ nm	240000	0.4 M Na_2S and 0.6 M Na_2SO_3	current work

Summarizing the information about the $\text{Cd}_x\text{Zn}_{1-x}\text{S}$ photocatalysts synthesized through various synthetic methods, reaction condition plays a key role in controlling the photocatalytic performance. It can be seen that neither calcination in high temperature nor coprecipitation in room temperature is positive to the enhancement of photocatalytic performance, because calcination in high temperature would lead to the formation of sintering while coprecipitation in room temperature usually obtains products in poor crystallinity. $\text{Cd}_x\text{Zn}_{1-x}\text{S}$ photocatalysts synthesized through hydro/solvothermal method usually exhibit good crystallinity, large specific surface

area and excellent photocatalytic performance. However, amount of products synthesized through hydro/solvothermal method is usually low because of the limitation of autoclave capacity. Compared with the other methods, microwave-assisted synthesis possesses many great advantages. The remarkable reaction rate could shorten the reaction time from hours to minutes and the amount of products could easily reach to gram-scale.

Reference

1. L. Bengtsson, *Physical Review B*, 1999, **59**, 12301.
2. M. C. Liu, L. Z. Wang, G. Q. Lu, X. D. Yao and L. J. Guo, *Energy Environ Sci*, 2011, **4**, 1372.
3. Y. G. Yu, G. Chen, L. X. Hao, Y. S. Zhou, Y. Wang, J. Pei, J. X. Sun and Z. H. Han, *Chem Commun*, 2013, **49**, 10142.
4. F. del Valle, A. Ishikawa, K. Domen, J. A. Villoria de la Mano, M. C. Sánchez-Sánchez, I. D. González, S. Herreras, N. Mota, M. E. Rivas and M. C. Álvarez Galván, *Catal Today*, 2009, **143**, 51.
5. J. Yu, J. Zhang and M. Jaroniec, *Green Chem*, 2010, **12**, 1611.
6. Q. Li, H. Meng, P. Zhou, Y. Q. Zheng, J. Wang, J. G. Yu and J. R. Gong, *ACS Catalysis*, 2013, **3**, 882.

Figure S1–S12

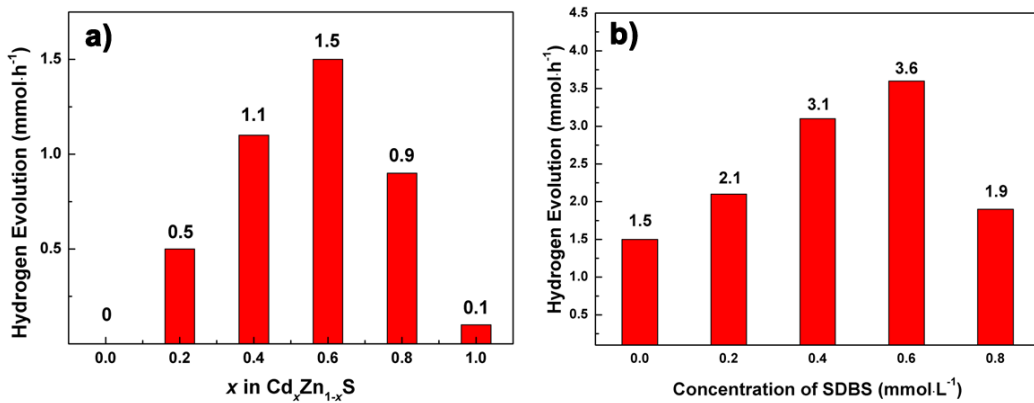


Fig. S1 H_2 evolution from an aqueous solution containing $0.6 \text{ mol}\cdot\text{L}^{-1}$ Na_2SO_3 and $0.4 \text{ mol}\cdot\text{L}^{-1}$ Na_2S catalyzed by a) $\text{Cd}_x\text{Zn}_{1-x}\text{S}$ photocatalysts ($x=0-1$) and b) $\text{Cd}_{0.6}\text{Zn}_{0.4}\text{S}$ photocatalysts synthesized with variable concentration of SDBS.

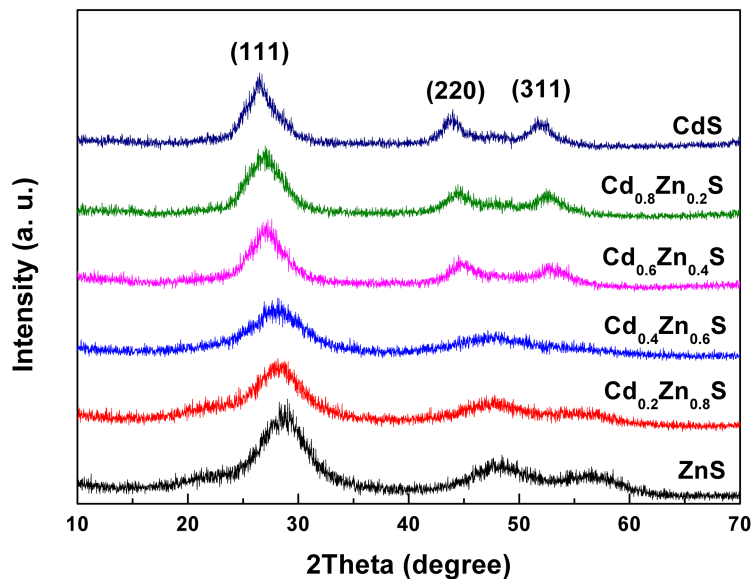


Fig. S2 XRD patterns of $\text{Cd}_x\text{Zn}_{1-x}\text{S}$ solid solution ($x=0-1$). Diffraction peaks of pure CdS and ZnS can be indexed to CdS (JCPDS No. 65-2887) and ZnS (JCPDS No. 65-0309) indicating both of CdS and ZnS synthesized though this route are cubic sphalerite structure.

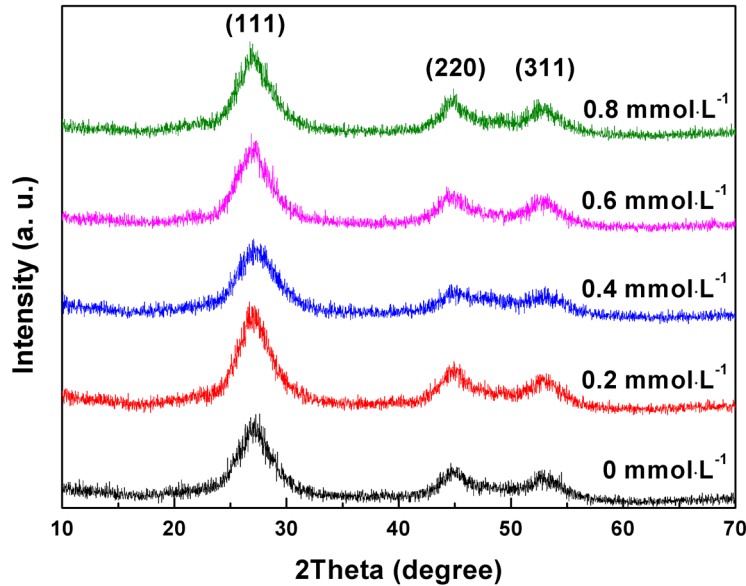


Fig. S3 XRD patterns of Cd_{0.6}Zn_{0.4}S photocatalysts synthesized with variable concentration of SDBS.

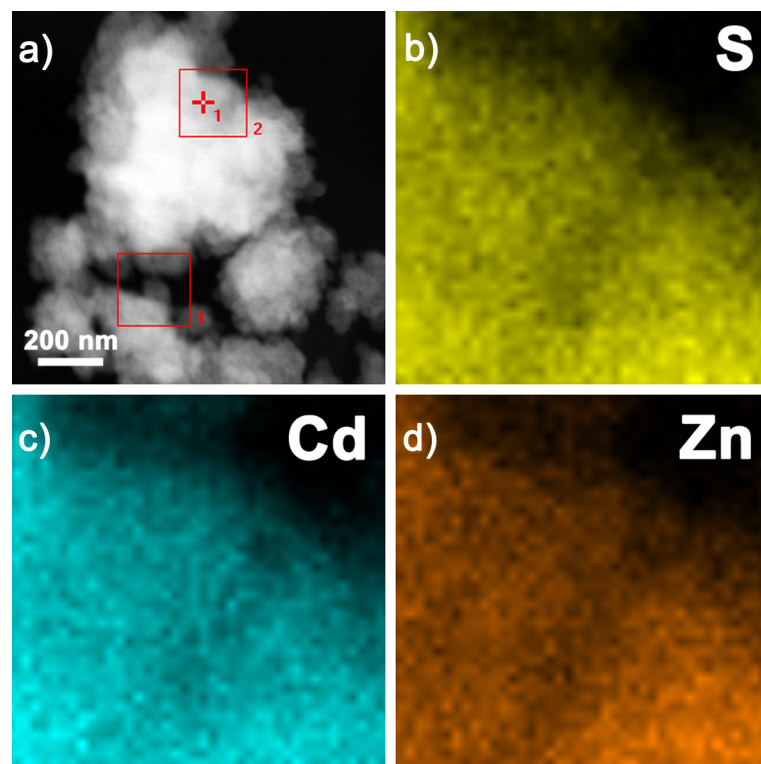


Fig. S4 The XEDS analysis results of Cd_{0.6}Zn_{0.4}S-0.6 photocatalyst: a) HAADF image and XEDS energy mapping of b) S (yellow), c) Cd (cyan) and d) Zn (orange). The XEDS spectra were acquired at a probe dwell time of 2 s and step size of 5 nm to distinguish spatial uniformity of the elemental distribution.

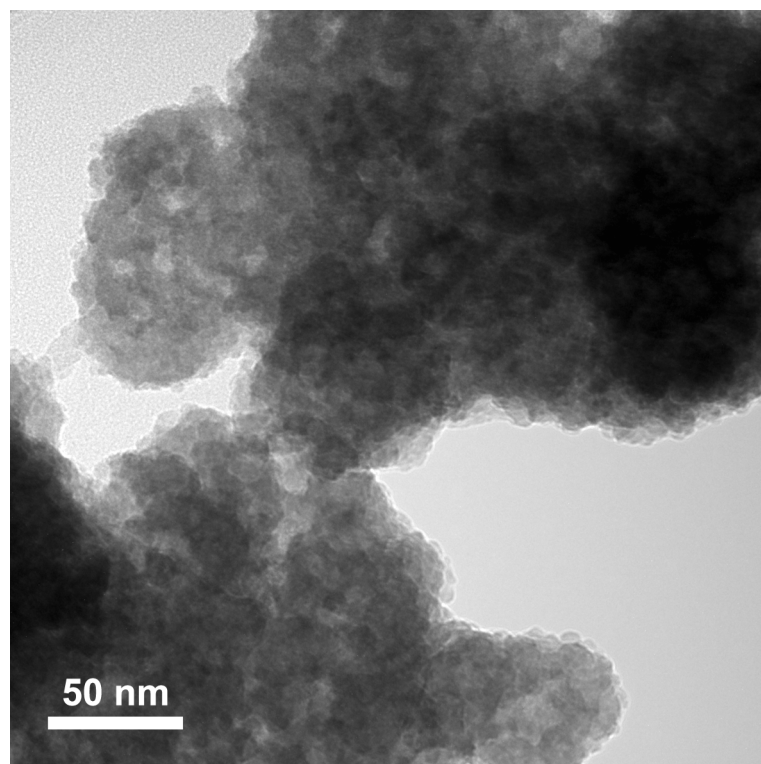


Fig. S5 TEM image of porous structure in $\text{Cd}_{0.6}\text{Zn}_{0.4}\text{S}-0.6$ photocatalyst. Wormhole-like mesopores can be found in the self-assembled structures with the diameter between 3 and 10 nm.

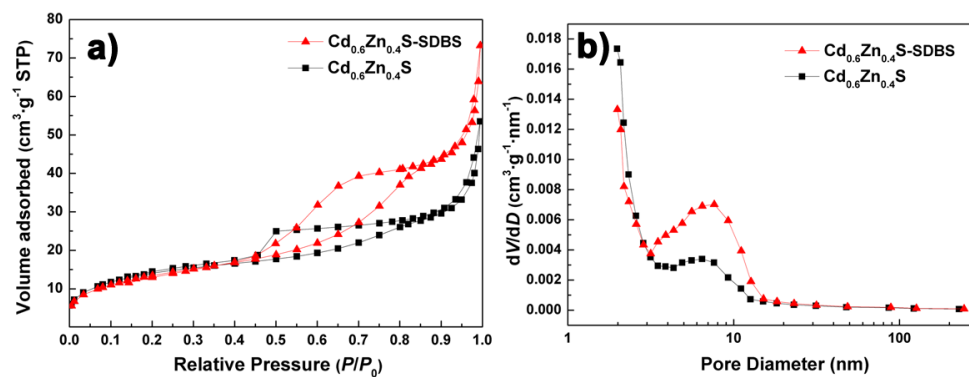


Fig. S6 Nitrogen adsorption/desorption isotherms and (b) pore size distribution curves of $\text{Cd}_{0.6}\text{Zn}_{0.4}\text{S}$ solid solution synthesized in the absence of SDBS and in the presence of $0.6 \text{ mmol} \cdot \text{L}^{-1}$ SDBS. The pore-size distribution curves show that the pore sizes of both $\text{Cd}_{0.6}\text{Zn}_{0.4}\text{S}$ solid solutions synthesized in the absence of SDBS and in the presence of $0.6 \text{ mmol} \cdot \text{L}^{-1}$ SDBS are also concentrated between 3 and 10 nm.

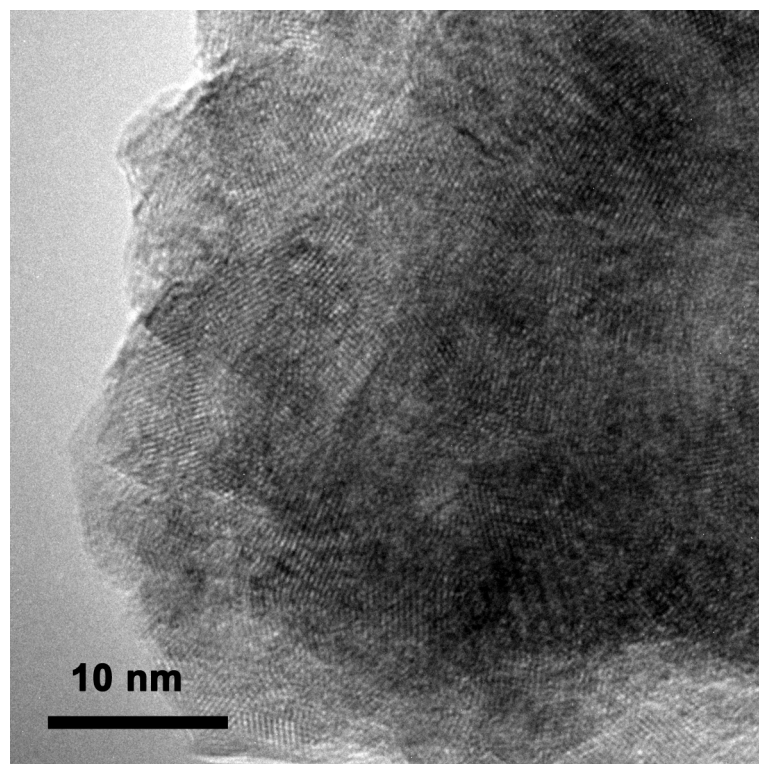


Fig. S7 HRTEM image of Cd_{0.6}Zn_{0.4}S photocatalyst prepared without SDBS.

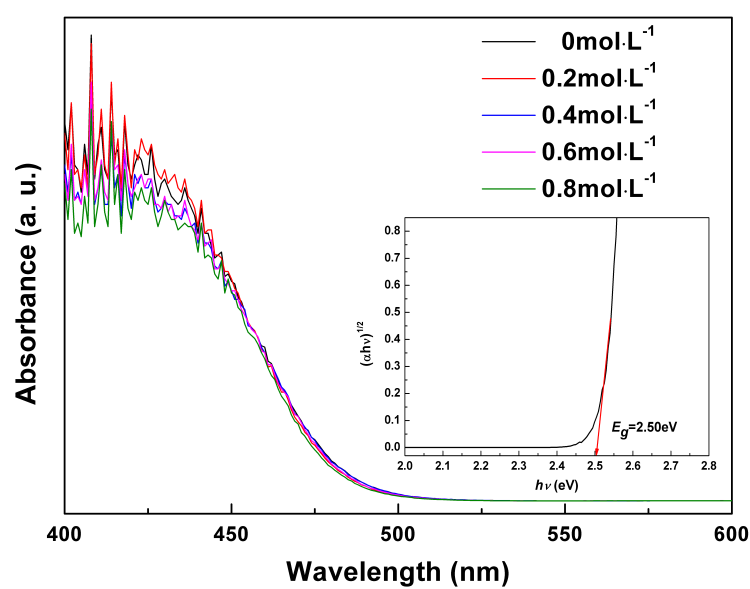


Fig. S8 UV-vis absorption spectra for Cd_{0.6}Zn_{0.4}S solid solution synthesized with variable amount of SDBS. The inset is the representative tauc plot of Cd_{0.6}Zn_{0.4}S-0.6 photocatalyst.

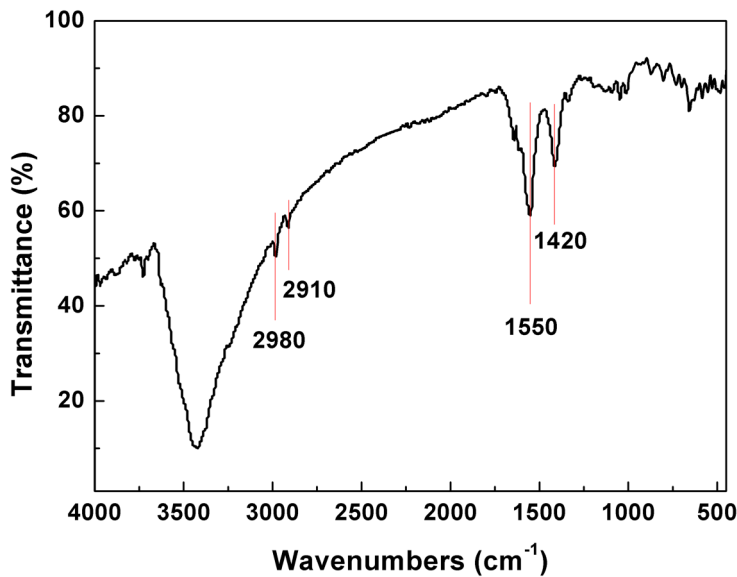


Fig. S9 FT-IR spectra of Cd_{0.6}Zn_{0.4}S photocatalyst synthesized with 0.8 mmol·L⁻¹ SDBS.

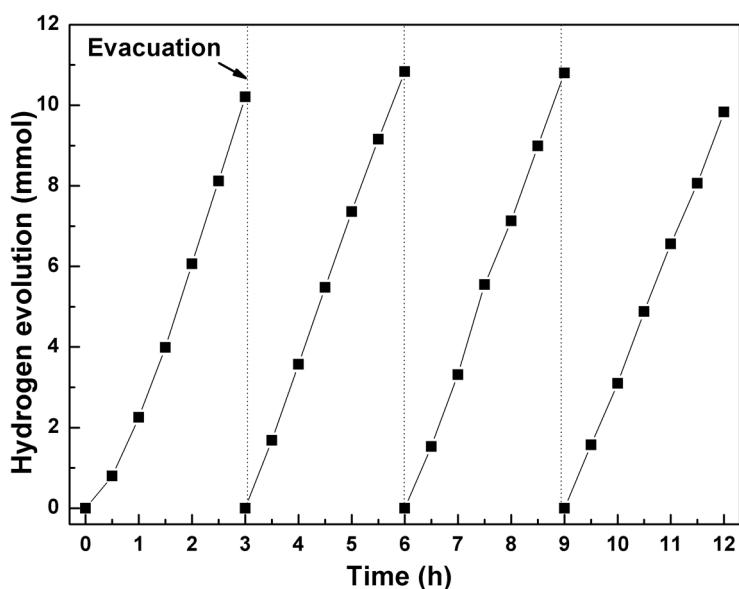


Fig. S10 Amount of H₂ evolution according to reaction time for Cd_{0.6}Zn_{0.4}S photocatalyst.

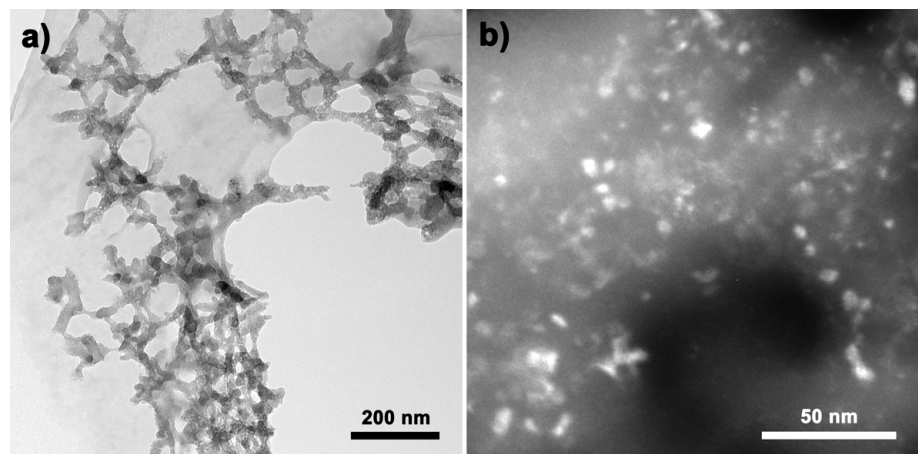


Fig. S11 a) TEM image and b) dark field image of $\text{Cd}_{0.6}\text{Zn}_{0.4}\text{S}-0.6$ sample after photocatalytic reaction for 2h.

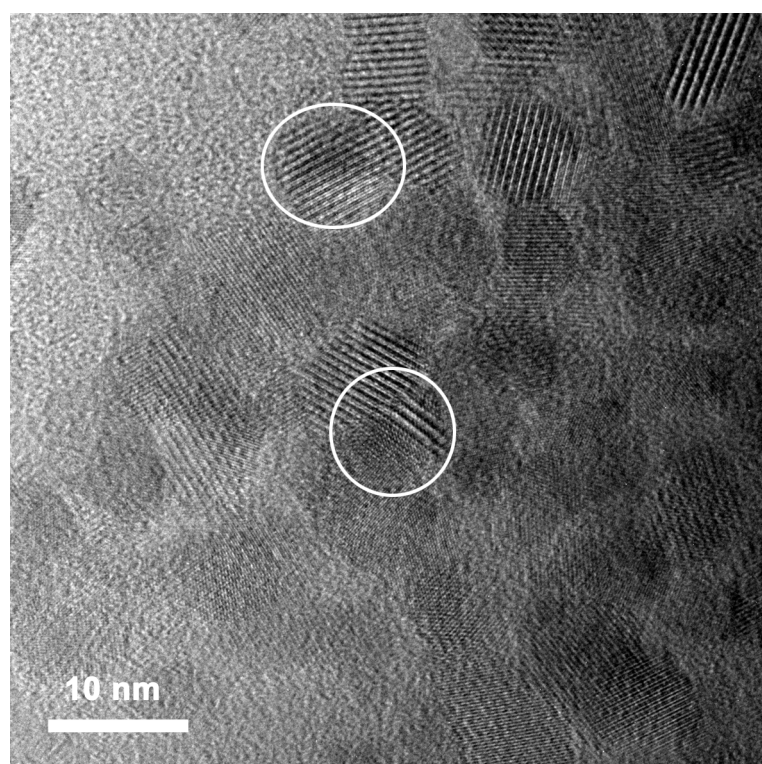


Fig. S12 HRTEM image of $\text{Cd}_{0.6}\text{Zn}_{0.4}\text{S}-0.6$ sample after photocatalytic reaction for 2h.
Nanocrystals with twin structure were marked with white circles.